

FEM-Based Simulation of a Brushless Motor Behavior for Different Supplying Strategies

Adrian MUNTEANU, Alecsandru SIMION, Leonard LIVADARU

"Gheorghe Asachi" Technical University of Iasi

Bd. D. Mangeron, No. 51-53, 700050 Iasi, ROMANIA

amunteanu@ee.tuiasi.ro, asimion@ee.tuiasi.ro, livadaru@ee.tuiasi.ro

Abstract—This paper presents the FEM based simulation results of a brushless motor behavior for different supplying strategies. The motor structure that has been considered for the simulation combines the specific elements of classic BLDC, SRM and stepper motor. Only open-loop commutation strategies (no feedback on the rotor position) have been taken into discussion. A major attention was given to speed evolution during start-up and load variation operation, and torque ripple for each situation.

Index Terms—brushless motor, FEM simulation, open-loop commutation, permanent magnet, torque ripple

I. INTRODUCTION

Electric motors come in a rich variety of configurations to suit different purposes. Multiple advantages brought by brushless motors development (high power density and efficiency, absence of brushes that ensures high reliability, less acoustic and electrical noise, lower maintenance costs, safe operation in dangerous environment, and the variety of the control modes) led to enlarging the application domain of these motor types and justifies the high interest of the researchers on these topics.

Brushless motors differ in terms of motor type and phase-number. There are three choices for motor type: AC, DC, and stepper. Brushless DC motors are used most often in variable speed and torque applications. Brushless AC motors include both synchronous and induction products. Brushless stepper motors provide incremental motion or steps in response to pulse of current that alternately change the polarity of the stator poles. Brushless stepper motors do not require feedback, and are used sometimes in open loop or no-feedback applications. In terms of phase-number, brushless motors include both single-phase motors and three-phase motors. Single-phase brushless motors are used in residential applications whereas three-phase brushless motors are designed for industrial use. Motor construction is an important specification to consider when specifying brushless motors.

II. MOTOR DESCRIPTION

The brushless motor discussed in this paper has SRM type geometry (Fig. 1), with different rotor and stator poles number (10/12). The rotor structure consists of 10 poles with single-layer interior permanent magnets (most common and also efficient design) in alternating polarity on the rotor extremity, while the stator electromagnetic poles are powered by means of 12 concentrated coils. The variable reluctance of the air gap is provided by the rotor poles shape.

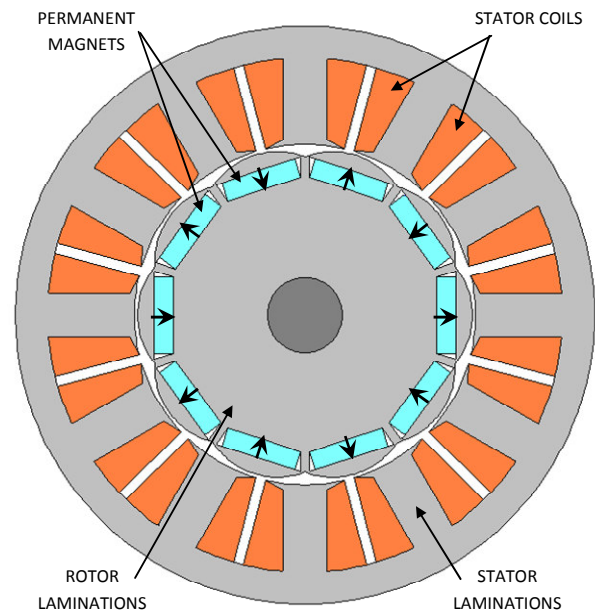


Fig. 1 Cross-section of the brushless motor

Table I presents constructive parameters of the brushless motor while Table II contains information referring to main electrical parameters.

TABLE I. CONSTRUCTIV PARAMETERS

Item	Value
Motor length	110 mm
Outer rotor diameter	52 mm
Outer stator diameter	90 mm
PM dimensions	3.5/12.5 mm
Minimum air gap length	0.5 mm
Stator coils	12
Rotor poles	10
Rated speed	1000 rpm

TABLE II. ELECTICAL PARAMETERS

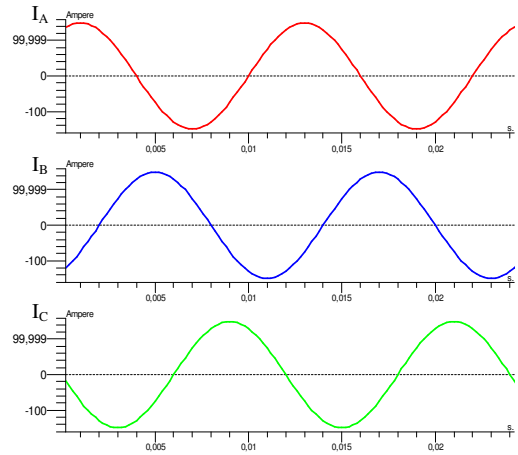
Item	Value
Stator	
Coil resistance	12 mΩ
Number of turns/coil	4
Rated current	150 A
Rotor	
PM magnetic remanence B_r	1.26 T
PM coercive field strength H_c	1650 A/m

As concerning the stator windings, the 12 concentrated coils, with distinctive accessible terminals, can easily be connected in order to create different poles distribution, when the analyzed supplying strategies are applied.

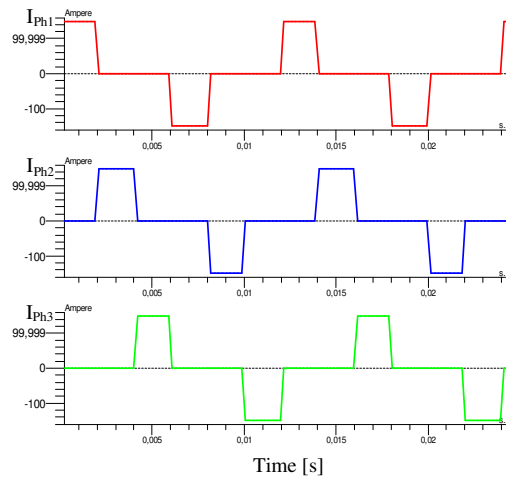
III. SUPPLYING STRATEGIES

- Two different supplying strategies were applied (Fig. 2):
- the first one uses a sinusoidal three phase supplying system – case A,
 - the other one uses three rectangular current impulses – case B and case C.

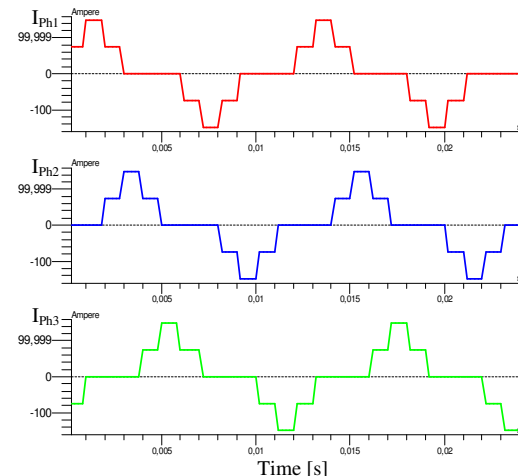
For each one, it has been accomplished different connections of the 12 stator coils in order to obtain the desired poles distribution. The four considered distinctive situations are presented in Fig. 3 cases I and II for the sinusoidal three phase supplying system and cases III and IV for the rectangular current control strategies.



Case A

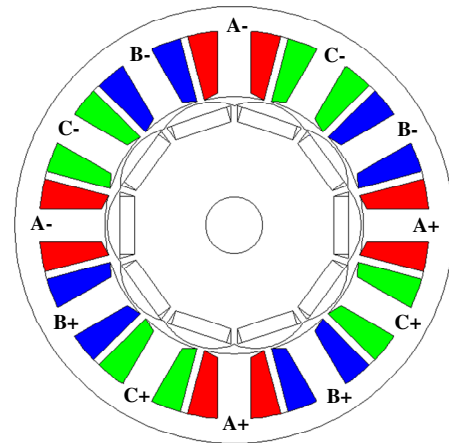


Case B

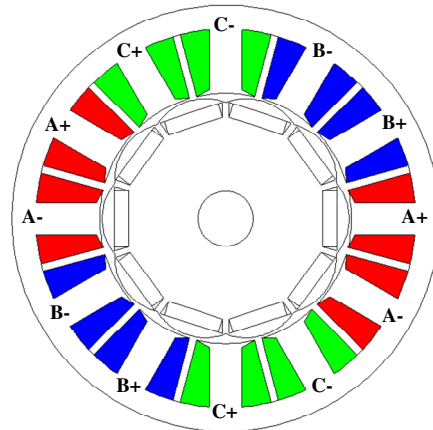


Case C

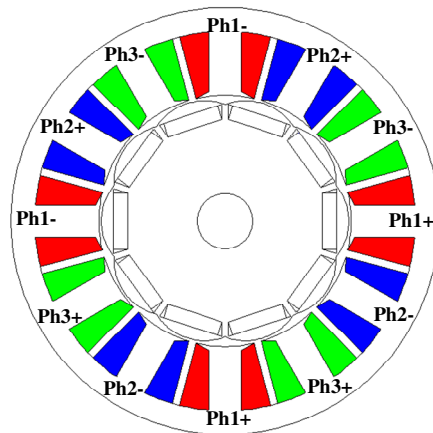
Fig. 2 Phase currents



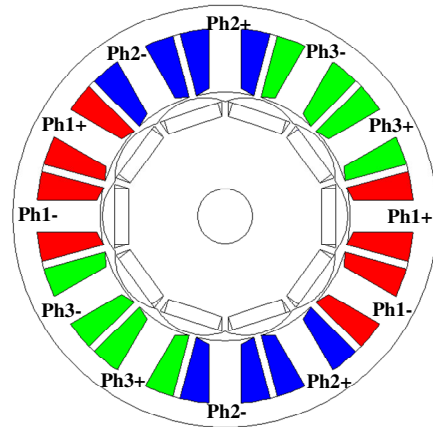
Case I



Case II



Case III



Case IV

Fig. 3 Phases distribution

IV. FEM BASED SIMULATION APPROACH

For this study, the FEM-based analysis took into consideration a 2D model approach, knowing the geometrical symmetry of the electrical machine along axial length (any cross-section is representative for the entire structure). The simulation consisted in a transient magnetic analysis, which allows us to analyze a rotating machine taking into account the motion of the rotor. At each time step the position, the velocity and the acceleration of the rotor are determined solving the kinematic equation (1):

$$J\ddot{\theta} = C_m - f\dot{\theta} - C_r - k(\theta - \theta_0) \quad (1)$$

where:

- J = moment of inertia;
- f = coefficient of viscous friction;
- C_m = magnetic torque;
- C_r = resistive torque;
- $\ddot{\theta}$ = angular acceleration;
- $\dot{\theta}$ = angular velocity;
- k = torsion constant;
- θ = current angular position of the spring;
- θ_0 = angular position of the spring at reset.

Table III contains the defined quantities for the studied brushless motor.

TABLE III. MECANICAL QUANTITIES

Item	Value
Moment of inertia – J	$0.6 \cdot 10^{-3} \text{ kg} \cdot \text{m}^2$
Coefficient of viscous friction – f	$0.02 \text{ N} \cdot \text{m} \cdot \text{s}$
Resistive torque – C_r	$0 \div 8 \text{ N} \cdot \text{m}$
Torsion constant of the spring – k	$0.1 \cdot 10^{-4} \text{ N} \cdot \text{m}$
Rest position – $\theta - \theta_0$	0 degrees

In a transient magnetic problem the solving process consists of a sequence of solving processes carried out in time (called time step). The temporal equation is a first order differential equation and it is integrated by an implicit method. Thus, all the quantities are computed for the final time value of each time step.

The time step value has to be chosen carefully, function of the time constant of the modeled system, the periodicity of the sources and the rotating speed of the machine. In our case, the time step value is $\Delta t = 0.0002 \text{ s}$, which ensures 60 steps on a period of the source ($T = 0.012 \text{ s}$) and 300 steps on one complete rotor revolution.

V. RESULTS AND DISCUSSIONS

Different operating conditions have been simulated for all considered cases (case I-A – phases distribution I and supplying strategy A, case II-A – phase distribution II and supplying strategy A, case III-B – phase distribution III and supplying strategy B, case IV-B – phase distribution IV and supplying strategy B, case III-C – phase distribution III and supplying strategy C, case IV-C – phase distribution IV and supplying strategy C).

Speed evolution for no-load start-up process and oscillations caused by a 6 Nm load torque are presented in Fig. 4. As regards the start-up process, which takes less then 0.3 seconds, the speed has similar evolutions for all cases.

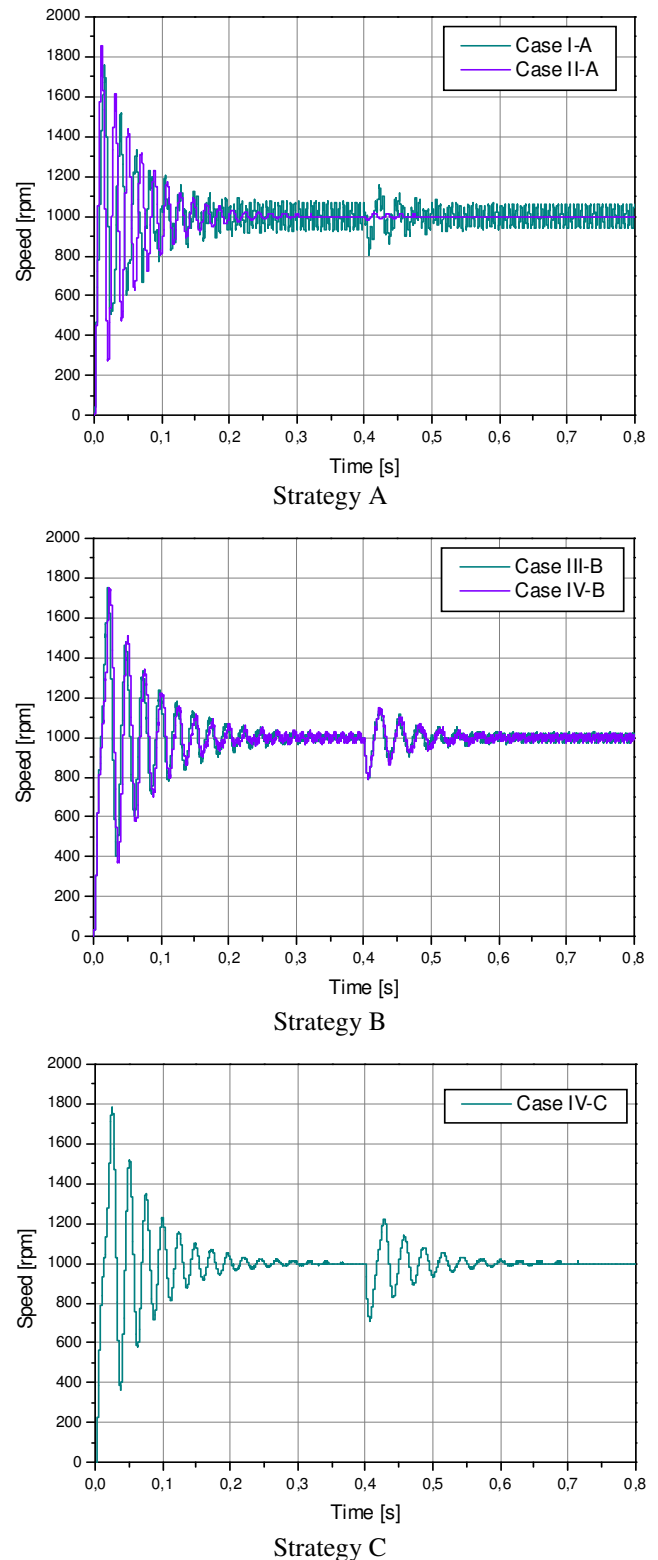


Fig. 4 Speed variation

It can not be told the same thing about the steady-state operation when, the speed oscillations have significant different amplitudes. Case I-A generates the highest oscillations. Better results are obtained for supplying strategy B. The best behavior of the brushless motor is achieved for case II-A and case IV-C, when the speed is almost constant (insignificant oscillations). The difference between these two cases consists in the perturbation level produced by applying the load, which is higher for the last situation.

The same conclusion can be restated comparing the two corresponding magnetic torque characteristics (Fig. 5).

As concerns the case III-C, the results show that the supplying strategy applied to this phase configuration is not capable to ensure an appropriate torque value for the start-up process.

An important evaluation for brushless motors is the predicted cogging torque, presented in Fig. 6. It can be easily observed the major differences of the motor behavior for the analyzed cases. On the basis of these dependences, the more appropriate supplying strategy for a given electric drive can be chosen.

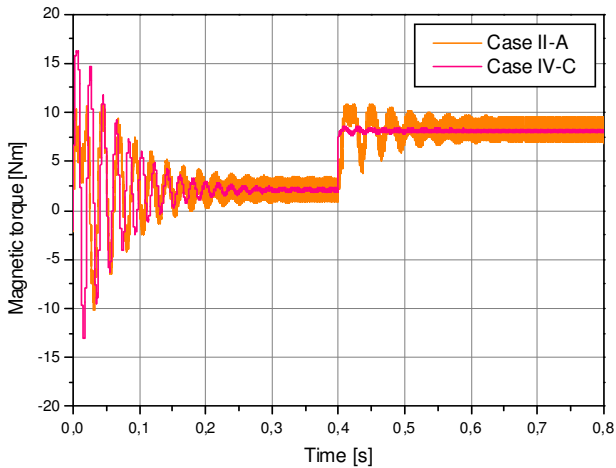
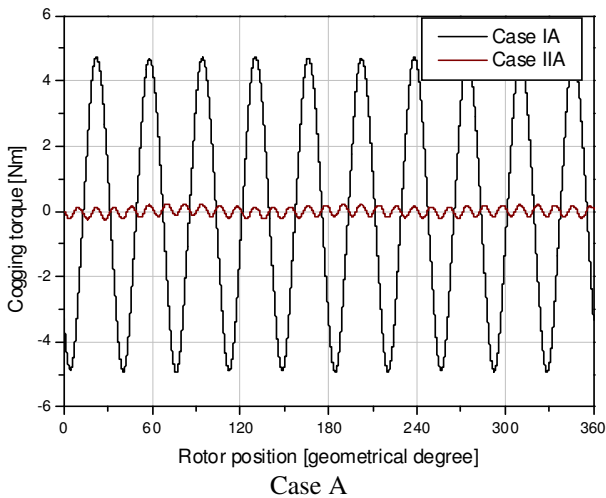
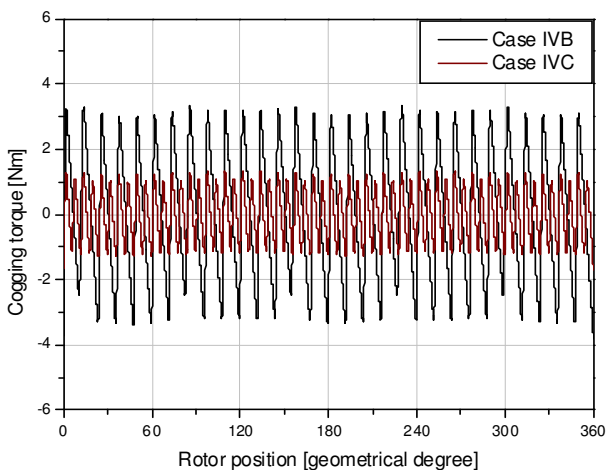


Fig. 5 Magnetic torque characteristics



Case A



Case IV

Fig. 6 Cogging torque

Once more it is confirmed that case II-A has the lower cogging torque and speed oscillations, but satisfactory results are achieved for case IV-C as well. Both situations can be used as good supplying strategies.

VI. CONCLUSION

The use of the FEM based simulation approach represents a truthfully method in predicting the behavior of any brushless motor for different supplying strategies.

Speed and torque evolutions for different transient regimes can be used in deciding the most appropriate solution for a certain application.

For our case, the best results, regarding the speed evolution and torque ripple are achieved for using the three phase sinusoidal current system and a neighborly distribution of the alternating stator poles.

The strategy based on three rectangular current impulses on different poles distribution leads to an increasing of the speed oscillations and torque ripple, but ensures an easier control of the machine. Better results are achieved using strategy C, when at certain moments two phases are supplied simultaneously.

For a complete analysis of the brushless motor behavior, a more complete model, that includes a feedback on the rotor position, is necessary. This model is presently under construction.

REFERENCES

- [1] Z. Q. Zhu, J. T. Chen, Y. Pang, D. Hower, S. Iwasaki and R. Deodhar, "Analysis of a Novel Multi-Tooth Flux-Switching PM Brushless AC Machine for High Torque Direct-Drive Applications", *IEEE Trans Mag.*, vol. 44, no. 11, pp. 4313-4316, Nov. 2008.
- [2] K. Atallah, J. Renu, S. Mezani and D. Howe, "A Novel Pseudo Direct-Drive Brushless Permanent Magnet Machine", *IEEE Trans Mag.*, vol. 44, no. 11, pp. 4349-4352, Nov. 2008.
- [3] J. Junak, G. Ombach, "Comparison of permanent magnet brushless motors designed for Automated Manual Transmission (AMT) systems", *Conference on Electrical Machines and Systems, ICEMS 2008*, pp. 2773-2777, Oct. 2008.
- [4] C. G. Kim, J. H. Lee, H. W. Kim, M. J. Youn, "Study on maximum torque generation for sensorless controlled brushless DC motor with trapezoidal back EMF", *IEE Proc. of Electric Power Applications*, vol. 152, no. 2, pp. 277-291, March 2005.
- [5] Y. S. Chen, Z. Q. Zhu, "Investigation of Magnetic Drag Torque in Permanent Magnet Brushless Motors", *IEEE Trans Mag.*, vol. 43, no.6, pp. 2507-2509, June 2007.
- [6] J. F. Gieras, "Analytical approach to cogging torque calculation of PM brushless motors", *IEEE Trans. Ind. Appl.*, vol. 40, no. 5, pp. 1310-1316, Sept.-Oct. 2004.
- [7] T. Marcic, G. Stumberger, B. Stumberger, M. Hadziselimovic and P. Vrtic, "Determining Parameters of a Line-Start Interior Permanent Magnet Synchronous Motor Model by the Differential Evolution", *IEEE Trans Mag.*, vol. 44, no. 11, pp. 4385-4388, Nov. 2008.
- [8] P. S. Shin, S. H. Woo, Y. Zhang and C. S. Koh, "An Application of Latin Hypercube Sampling Strategy for Cogging Torque Reduction of Large-Scale Permanent Magnet Motor", *IEEE Trans Mag.*, vol. 44, no. 11, pp. 4421-4424, Nov. 2008.
- [9] M. Bonfe, M. Bergo, "A brushless motor drive with sensorless control for commercial vehicle hydraulic pumps", *IEEE International Symposium on Industrial Electronics, ISIE 2008*, pp.612-617, June-July 2008.
- [10] R. Krishnan, *Switched Reluctance Motor Drives – Modeling, Simulation, Analysis, Design and Applications*, CRC Press LLC – U.S.A., 2001.
- [11] I. Boldea, *Reluctance Synchronous Machines and Drives*, Clarendon Press, Oxford, 1996.
- [12] E. Dariu, "The Production of a Ripple Free Torque in Switched Reluctance Motor Drives", *Bul. Inst. Polit., Tomul LII (LVI)*, Fasc. 5A, pp. 281-286, 2006.